The Impact of the 'Austrian' Mutation of the Amyloid Precursor Protein Transmembrane Helix is Communicated to the Hinge Region

Walter Stelzer[a], Christina Scharnagl[b], Ulrike Leurs[c], Kasper D. Rand[c], and Dieter Langosch*[a]

Abstract: The transmembrane helix of the amyloid precursor protein is subject to proteolytic cleavages by γ-secretase at different sites resulting in Aβ peptides of different length and toxicity. A number of point mutations within this transmembrane helix alter the cleavage pattern thus enhancing production of toxic Aβ peptide species that are at the root of familial Alzheimer's disease. Here, we investigated how one of the most devastating mutations, the 'Austrian' mutation T43I, affects this transmembrane helix. Site-resolved deuterium/hydrogen amide exchange experiments reveal that the mutation destabilizes amide hydrogen bonds in the hinge which connects dimerization and cleavage regions. Weaker intrahelical hydrogen bonds at the hinge may enhance helix bending and thereby affect recognition of the transmembrane substrate by the enzyme and/or presentation of its cleavage sites to the catalytic cleft.

Proteins exhibit a hierarchy of motions that range from local ones, such as side-chain rotations and the opening and closing of hydrogen bonds (H-bonds), to large-amplitude, correlated backbone motions. The functional relevance of these global modes, which allow proteins to access alternative conformations via cooperative structural changes, was confirmed for enzymatic catalysis, protein-protein binding etc. [1]. One interesting question is how local structural fluctuations define global backbone dynamics [2]. This is connected to the question how disease-causing mutations can affect protein stability and dynamics via changing the physico-chemical properties of particular residues [3]. Such issues appear pertinent to soluble and membrane proteins alike [4].

There is increasing interest in how the helical transmembrane domains (TMDs) of substrate proteins are recognized and cleaved by their cognate intramembrane proteases such as γ-secretase [5]. It was proposed that the transmembrane helices of substrates would require a flexible hinge at some distance from the actual cleavage sites. For example, a hinge has been identified at the $G_{37}G_{38}$ motif within the TMD of the γ-secretase substrate amyloid precursor protein (APP) [6]. This hinge connects a conformationally flexible dimerization domain, termed TM-N, to a surprisingly rigid cleavage domain, TM-C [6b]. In another recently reported substrate/enzyme system, the $N_{501}P_{502}$ motif forms a hinge within the TMD of the sterol regulatory element-binding protein, a substrate of site-2-protease. This NP motif localizes downstream of a rigid cleavage site [7]. In both cases, these hinges are located several helical turns away from the initial cleavage sites; therefore, motions at the hinges may modulate substrate binding and/or presentation of the scissile bond to the active site of the enzyme [5].

Proteolysis of APP by β-secretase and γ-secretase produces a mixture of Aβ peptides that are thought to generate the toxic oligomers and plaques causing Alzheimer's disease (AD) [8]. Natural point mutations within the APP TMD that are associated with familial AD (FAD) can increase the toxicity of the Aβ peptide mixture by increasing the Aβ42/Aβ40 ratio [9]. For example, the T43I ('Austrian') mutation (Aβ numbering) is thought to lead to an extremely early mean age-of-onset (36 y) by strongly increasing the Aβ42/Aβ40 ratio [10]. The side-chain of T43 is H-bonded to the main chain carbonyl oxygen of V39 and controls the repertoire of TM-N *versus* TM-C bending motions as indicated by molecular dynamics (MD) simulations [6d]. It is unclear, however, how the loss of this H-bond in the disease-causing T43I mutant is connected to the flexibility of the hinge.

Here, we investigated the effects of the T43I mutation on synthetic peptides representing the complete predicted APP TMD helix (A28-55 wild-type and T43I) (Fig. 1 A) in 80% (v/v) trifluoroethanol (TFE) /water. Due to the similar polarities of TFE (ε = 8.55) and protein interiors (ε ~4 to ~12 corresponding to dry and internally solvated proteins, respectively [11]) we consider 80% TFE as a reasonable mimic of the aqueous environment within the catalytic cleft of presenilin [12] as done previously [6b, 6d, 13]. Presenilin represents the catalytic subunit of γ-secretase.

Circular dichroism (CD) spectroscopy initially showed that wild type A28-55 forms ~80% helix in this solvent while the helicity of the T43I mutant is slightly decreased in favor of random coil (Fig. S1). Amide deuterium/hydrogen exchange (DHX) kinetics of exhaustively (> 95%) deuterated TMDs were recorded to compare the conformational equilibria along the wild-type and T43I helices. At a concentration of 5 µM the peptide remains monomeric [6b]. Under 'quenched conditions' (pH 2.5, 0°C), where the much more labile deuteriums bound to polar and non-H-bonded atoms quickly exchange for protons, both wild-type and T43I retain ~22 of the 27 backbone amide deuteriums that have the potential to form intrahelical H-bonds. The kinetics were then recorded at 20°C and pH 3 where fast exchange events can be monitored with higher precision than at elevated pH values. As exemplified by spectra shown in Fig. S2, the isotope envelopes gradually shift with incubation time towards lower mass/charge values. A gradual mass shift is diagnostic of uncorrelated exchange in the EX2 regime indicating transient local unfolding events [14].

[a] W. Stelzer, Prof. Dr. D. Langosch
Lehrstuhl Chemie der Biopolymere, Technical University of Munich and Munich Center for Integrated Protein Science (CIPS^M)
Weihenstephaner Berg 3, 85354 Freising (Germany)
*E-mail: langosch@tum.de
[b] Dr. C. Scharnagl
Fakultät für Physik E14, Technical University of Munich
Maximus-von-Imhof-Forum 4, 85354 Freising (Germany)
[c] Dr. U. Leurs, Prof. Dr. Kasper D. Rand
Department of Pharmacy, University of Copenhagen
Universitetsparken 2, 2100 Copenhagen (Denmark)

Supporting information for this article is given via a link at the end of the document.

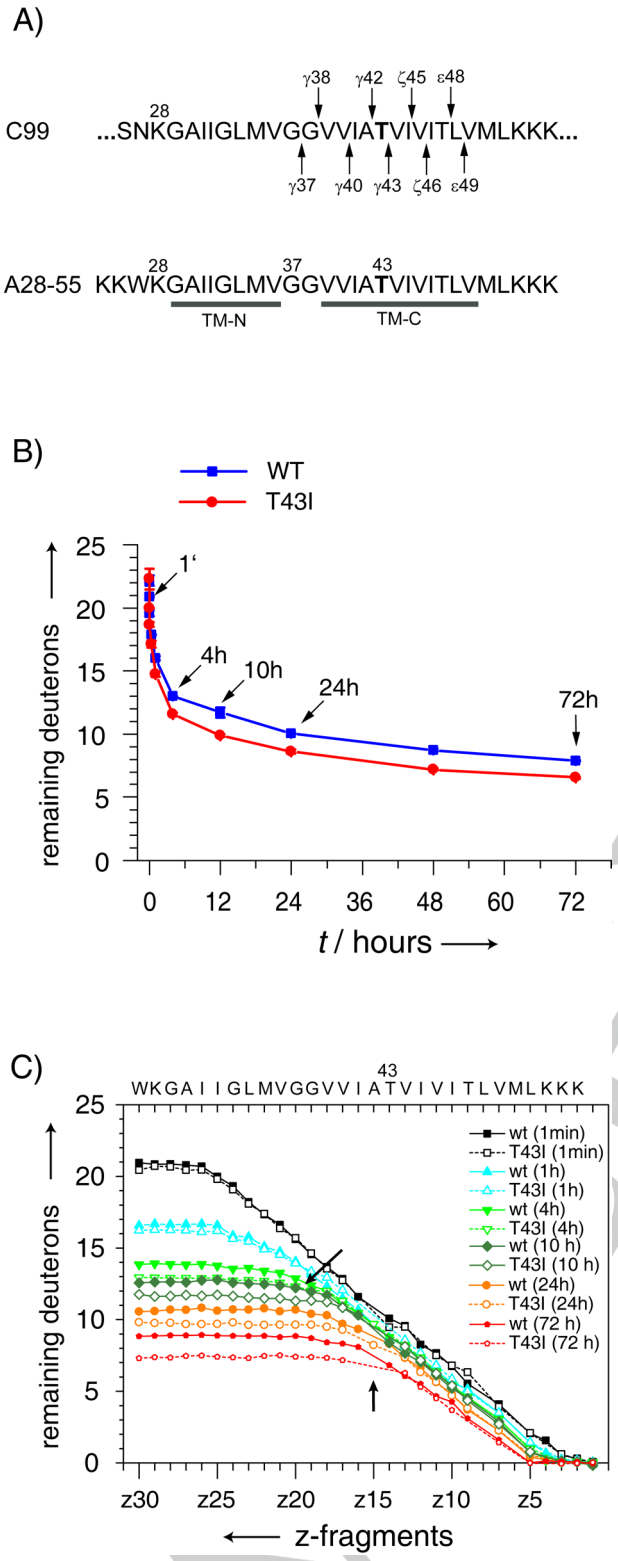

Figure 1. Amide DHX kinetics and site-specific exchange. (A) Sequences of the predicted APP TMD (Aβ numbering, arrows indicate cleavage sites recognized by γ-secretase) and the model peptides used here (A28-55 wild-type and its T43I mutant). All peptides contain an additional N-terminal KKW tag for better solubility and photometric quantification. (B) Overall DHX kinetics recorded from the masses of triply charged ions (n = 3, standard errors are smaller than the sizes of the symbols). (C) Deuterium contents of z-fragments aligned against sequence as determined after ETD (n = 3, SEM ≤0.1 deuteriums) done at different incubation periods (arrows in part B). A given position in the primary structure aligns with the z-ion type containing the respective amide proton or deuterium. Arrows signify sequence positions were deuterium contents of wild-type and T43I fragments begin to deviate from each other. Note that the deuterium contents of T43I z-fragments appear to be slightly below (<1 D) those of wild-type z-fragments at around I31/I32 after 1 h of DHX. At 4 h, both series of fragments deviate from each other by ~1 D around G37/G38. The difference increases to ~1.5 D after 72 h around A42 (the site of deviation around A42 could not be determined unequivocally due to overlapping fragments in the mass spectra that prevent their identification in some cases).

A difference between wild-type and T43I of ~1 amide deuterium develops early on and increases to ~1.5 deuteriums at longer incubation times (Fig. 1 B) indicating a slightly different backbone flexibility. In order to localize the site(s) where this difference originates, we employed gas-phase fragmentation of 5+ charged precursor ions by electron transfer dissociation (ETD) after different periods of DHX (arrows in Fig. 1 B). ETD fragmentation occurs inherently without proton/deuterium scrambling[15] and produces a c- and z-fragment ion series that extend from a given sequence position towards the N- or C-terminus, respectively. Inspection of the deuterium content of sequential fragment ions can thus resolve the deuterium labelling pattern to individual amide sites in both A28-55 peptides (Fig. S2 C). Site-specific differences in the DHX kinetics between wild-type and mutant result in differing deuterium contents of the corresponding fragments (see Fig. S3 for explanation). Fig. 1 C shows the deuterium contents of the z-fragments that are aligned with the TMD sequence. A flat region indicates completed exchange while a steep region signifies retention of amide deuteriums due to much slower exchange. The plot reveals a transition from an N-terminal flat region into a steep region; this transition progresses with incubation time mainly from the N-terminus towards the center. A flat region also develops at the C-terminus, albeit much more slowly. Thus, amide DHX mainly progresses from the N-terminus across TM-N towards TM-C. After 72 h, the N-terminal half of the TMD has exchanged almost completely while about two helical turns from T43 to M51 still have resisted exchange. This confirms that the N-terminal Gly-rich TM-N is much more flexible than TM-C [6b]. Longer incubation periods were not tested since the exchange curve was essentially flat after 72 h (Fig. 1 B).

Importantly, the deuterium contents of T43I z-fragments start to deviate from those of wild-type z-fragments by ~1 deuterium mainly around the $G_{37}G_{38}$ motif (arrow in Fig. 1 C) after 4 h of DHX. This difference increases to ~1.5 deuteriums after 72 h around T43. From the masses of individual z-fragments the kinetics of successive deuterium loss were then calculated for G37, G38, V39, and the region from V40-V44 (where missing z-fragments prevented the calculation of site-specific exchange kinetics) (Fig. 2 A). From the kinetics, we calculated site-specific amide exchange rate constants (Fig. 2 B). Accordingly, the rate constants of the T43I mutant exceeds wild-type rate constants mainly at G38 (Fig. 2 B). Under EX2 conditions, site-specific exchange rates can be converted to f_{open}, the fraction of exposed amides at the respective position, by considering the theoretical intrinsic (chemical) exchange rate constants in the unfolded state (k_{ch}) (see Experimental Section, ref. [16]). Note that f_{open} is equal to the inverse of the protection factor. Calculation of f_{open} was done for a standard situation of exchange in pure water.

The absolute values obtained for f_{open} are very likely an underestimation due to a number of factors given in the Experimental Section. Nonetheless, these factors influence DHX of both TMDs in a similar fashion thus allowing their comparison. The result reveals that f_{open} values at G37, G38, and V39 of T43I indeed exceed the respective values of the wild-type with non-overlapping error bars (Fig. 2 C, arrows).

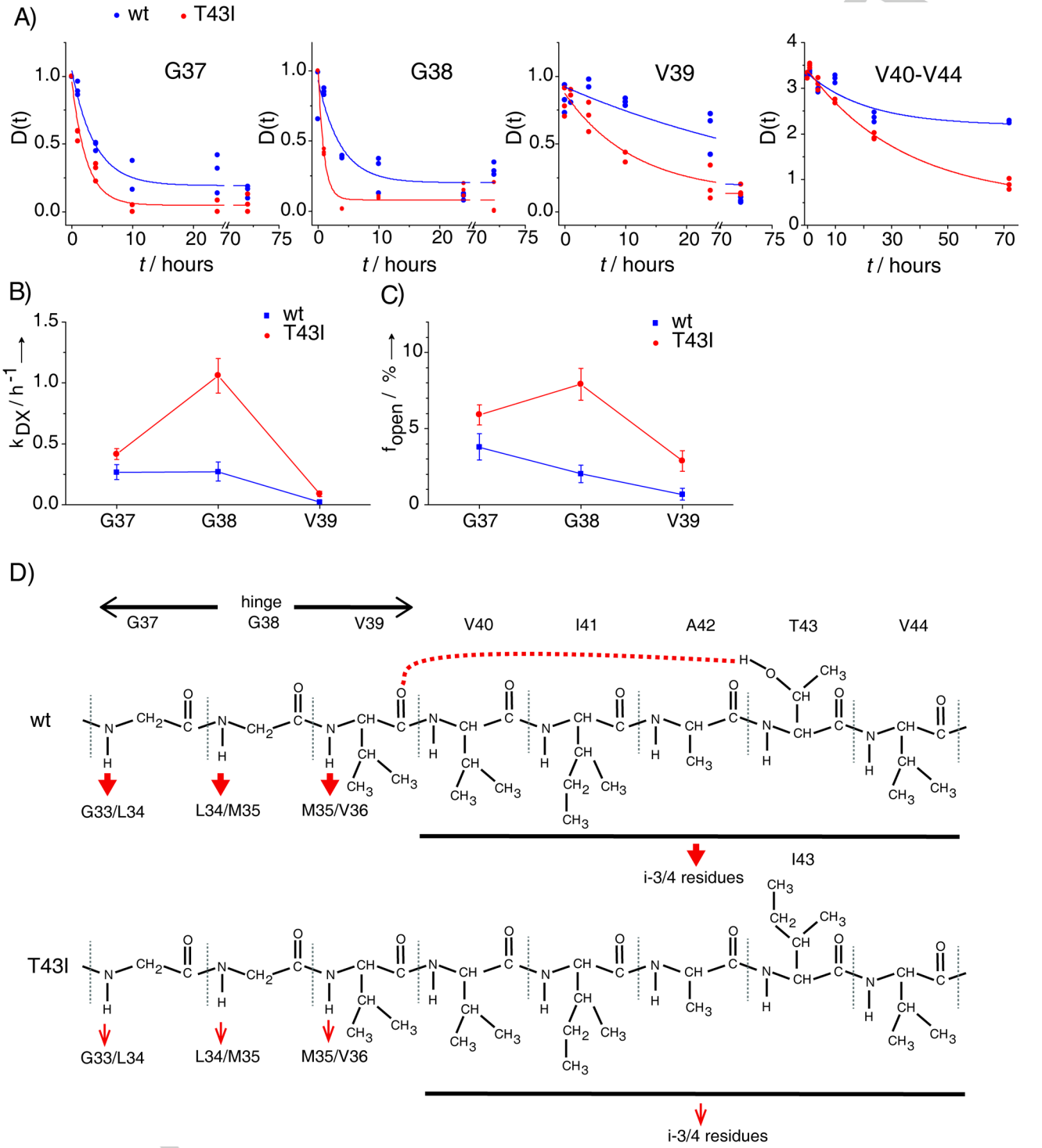

Figure 2. Site-specific DHX rates and fraction of exposed amides calculated from the deuterium contents of z-fragments. (A) The time-dependent loss of deuteriums at the indicated amides was fit to a first-order exchange kinetics and reveals acceleration of DHX at G37, G38, V39, and V40-V44 for the T43I mutant compared to wild-type. (B) Site-specific DHX rates from G37 to V39 as calculated from the curve fits in part A. (C) Site-specific fractions f_{open} of exposed amides calculated as the ratio of the exchange rates from the experiment (part B) and the calculated chemical exchange rates (k_{ch}) of exposed amides in a random coil structure. Note that f_{open} values of T43I at G37, G38, and V39 are enhanced relative to those of the wild-type TMD with non-overlapping error bars. (D)

Illustration showing how the loss of the side-chain/main-chain H-bond between the hydroxyl at position 43 and the V39 carbonyl reduces the stability of the amide H-bonds, reflected by the width of the arrows, that extend from V40 to V44 and from G37, G38, and V39 to their respective i-3 and i-4 partners.

Exchange kinetics are given for all residues where the corresponding z-fragments could be identified directly or determined by interpolation as detailed in the Experimental Section (Fig. S4). Exchange rate constants (Fig. S5) and f_{open} (Fig. S6) were determined in those cases where the data could be reliably fit by an exponential function. For residues other than those illuminated in Fig. 2, differences between wild-type and T43I were either not detectable or below statistical significance. Potential differences between V44 and L52 may be obscured by the extremely slow exchange within this part of the helix.

In sum, the data show that the loss of the H-bond between the T43 side chain and the V39 main chain carbonyl oxygen in the T43I mutation has two effects. First, this loss destabilizes the helix around position 43. Second, it is communicated to the hinge where it destabilizes the amide H-bonds extending from G37, G38, and V39 towards the respective i - 4 (α-helical bonding) and/or i - 3 (3_{10} helix) positions (Fig. 2 D). MD simulations have previously revealed a mixture of α-helical and 3_{10}-helical H-bonding near the $G_{37}G_{38}$ hinge [6b].

Which implications do these findings have for the mechanism by which the FAD mutation T43I affects the cleavage of the APP TMD by presenilin, the catalytic subunit of γ-secretase? Intramembrane proteolysis of the APP transmembrane helix is initiated at alternate ε48 and ε49 sites and continued by cleavage via ζ- and γ-sites mainly along two product lines (Fig. 1 A). In the case of the wild-type APP, preferred initial proteolysis at ε49 mainly produces Aβ40, while Aβ38 and the more toxic Aβ42 represent minor species resulting from a less efficient initial proteolysis at ε48 [8]. In T43I, the reduced usage of the ε49 site increases the Aβ42/Aβ40 ratio [17]. How could our present findings explain this impact of T43I? Previous MD simulations showed that the loss of the T43 side-chain/main-chain H-bonding in a T43V mutant increases the relative movements of TM-N versus TM-C at the $G_{37}G_{38}$ hinge [6d]. Thereby, a very subtle local destabilization, as detected here by increasing amide exchange kinetics, can translate into profound changes of global helix dynamics. An altered repertoire of helix bending motions may modulate exposure of cleavage sites to the enzyme's active site. An altered exposure may reduce endoproteolysis at ε49 relative to that at ε48 thus increasing the Aβ42/Aβ40 ratio [5]. In addition, destabilization of amide H-bonds around the hinge may affect substrate recognition by γ-secretase as the T43I mutation is also known to decrease substrate/enzyme affinity as suggested by an elevated K_M value [17].

In sum, our results reveal accelerated amide DHX in T43I relative to the wild type TMD. We localize the accelerated DHX to sites at the hinge region. Our experimental measurements suggest mechanisms by which FAD mutations, such as T43I, may accelerate the development of Alzheimer's disease in affected patients.

Experimental Section

Experimental details of peptide synthesis, circular dichroism (CD) spectroscopy, deuterium/hydrogen exchange mass spectrometry (DHX) with electron transfer dissociation (ETD) and data evaluation are given as Supporting Information.

Acknowledgements

This work was supported by the Deutsche Forschungsgemeinschaft (LA699/20-1, SCH630/4-1), the Center of Integrative Protein Science Munich (CIPS^M), the Marie Curie Actions Programme of the E.U (Grant No. PCIG09-GA-2011-294214), and the Danish Council for Independent Research | Natural Sciences (Steno Grant No. 0602-02047B).

Keywords: Alzheimer's disease • Amyloid beta-peptides • deuterium/hydrogen exchange • mass spectrometry • transmembrane helix

[1] K. Henzler-Wildman, D. Kern, *Nature* **2007**, *450*, 964-972.
[2] L. Vuillon, C. Lesieur, *Curr. Opin. Struct. Biol.* **2015**, *31*, 1-8.
[3] T. G. Kucukkal, M. Petukh, L. Li, E. Alexov, *Curr. Opin. Struct. Biol.* **2015**, *32*, 18-24.
[4] I. Bahar, T. R. Lezon, A. Bakan, I. H. Shrivastava, *Chem. Rev.* **2010**, *110*, 1463-1497.
[5] D. Langosch, C. Scharnagl, H. Steiner, M. K. Lemberg, *Trends Biochem. Sci.* **2015**, *40*, 318-327.
[6] a) P. J. Barrett, Y. Song, W. D. Van Horn, E. J. Hustedt, J. M. Schafer, A. Hadziselimovic, A. J. Beel, C. R. Sanders, *Science* **2012**, *336*, 1168-1171; b) O. Pester, P. Barret, D. Hornburg, P. Hornburg, R. Pröbstle, S. Widmaier, C. Kutzner, M. Dürrbaum, A. Kapurniotu, C. R. Sanders, C. Scharnagl, D. Langosch, *J. Am. Chem. Soc.* **2013**, *135*, 1317-1329; c) T. Lemmin, M. Dimitrov, P. C. Fraering, M. Dal Peraro, *J. Biol. Chem.* **2014**, *289*, 6763-6774; d) C. Scharnagl, O. Pester, P. Hornburg, D. Hornburg, A. Götz, D. Langosch, *Biophys. J.* **2014**, *106*, 1318-1326.
[7] R. Linser, N. Salvi, R. Briones, P. Rovo, B. L. de Groot, G. Wagner, *Proc. Natl. Acad. Sci. U.S.A.* **2015**, *112*, 12390-12395.
[8] S. F. Lichtenthaler, C. Haass, H. Steiner, *J. Neurochem.* **2011**, *117*, 779-796.
[9] S. Weggen, D. Beher, *Alzheimers Research & Therapy* **2012**, *4*.
[10] a) S. Kumar-Singh, C. De Jonghe, M. Cruts, R. Kleinert, R. Wang, M. Mercken, B. De Strooper, H. Vanderstichele, A. Lofgren, I. Vanderhoeven, H. Backhovens, E. Vanmechelen, P. M. Kroisel, C. Van Broeckhoven, *Hum. Mol. Genet.* **2000**, *9*, 2589-2598; b) R. M. Page, A. Gutsmiedl, A. Fukumori, E. Winkler, C. Haass, H. Steiner, *J. Biol. Chem.* **2010**, *285*, 17798-17810; c) L. Chavez-Gutierrez, L. Bammens, I. Benilova, A. Vandersteen, M. Benurwar, M. Borgers, S. Lismont, L. Zhou, S. Van Cleynenbreugel, H. Esselmann, J. Wiltfang, L. Serneels, E. Karran, H. Gijsen, J. Schymkowitz, F. Rousseau, K. Broersen, B. De Strooper, *EMBO J.* **2012**, *31*, 2261-2274.
[11] C. N. Schutz, A. Warshel, *Proteins* **2001**, *44*, 400-417.
[12] C. Sato, Y. Morohashi, T. Tomita, T. Iwatsubo, *J. Neurosci* **2006**, *26*, 12081-12088.

[13] O. Pester, A. Götz, G. Multhaup, C. Scharnagl, D. Langosch, *Chem. Bio. Chem.* **2013**, *14*, 1943-1948.
[14] H. Xiao, J. K. Hoerner, S. J. Eyles, A. Dobo, E. Voigtman, A. I. Mel'Cuk, I. A. Kaltashov, *Prot. Sci.* **2005**, *14*, 543-557.
[15] K. D. Rand, C. M. Adams, R. A. Zubarev, T. J. Jorgensen, *J. Am. Chem. Soc.* **2008**, *130*, 1341-1349.
[16] a) S. W. Englander, *J. Am. Soc. Mass Spectrom.* **2006**, *17*, 1481-1489; b) J. J. Skinner, W. K. Lim, S. Bedard, B. E. Black, S. W. Englander, *Protein Sci.* **2012**, *21*, 996-1005.
[17] L. Chavez-Gutierrez, L. Bammens, I. Benilova, A. Vandersteen, M. Benurwar, M. Borgers, S. Lismont, L. Zhou, S. Van Cleynenbreugel, H. Esselmann, J. Wiltfang, L. Serneels, E. Karran, H. Gijsen, J. Schymkowitz, F. Rousseau, K. Broersen, B. De Strooper, *EMBO J.* **2012**, *31*, 2261-2274.
[18] B. Poschner, J. Reed, D. Langosch, M. W. Hofmann, *Analyt. Biochemistry* **2007**, *363*, 306-308.
[19] B. C. Poschner, S. Quint, M. Hofmann, D. Langosch, *J. Mol. Biol.* **2009**, *386*, 733-741.
[20] W. Stelzer, B. C. Poschner, H. Stalz, A. J. Heck, D. Langosch, *Biophys. J.* **2008**, *95*, 1326-1330.
[21] K. D. Rand, S. D. Pringle, M. Morris, J. R. Engen, J. M. Brown, *J. Am. Soc. Mass Spectrom.* **2011**, *22*, 1784-1793.
[22] K. D. Rand, S. D. Pringle, M. Morris, J. M. Brown, *Analytical Chemistry* **2012**, *84*, 1931-1940.
[23] K. Teilum, B. B. Kragelund, F. M. Poulsen, *Application of Hydrogen Exchange Kinetics to Studies of Protein Folding, Vol. Part I*, Wiley-VCH, Weinheim, **2005**.
[24] W. M. Hart-Cooper, C. Sgarlata, C. L. Perrin, F. D. Toste, R. G. Bergman, K. N. Raymond, *Proc. Natl. Acad. Sci. U. S. A.* **2015**, *112*, 15303-15307.

Entry for the Table of Contents
Layout 1:

COMMUNICATION

The ‘Austrian’ mutation T43I within the transmembrane helix of the amyloid precursor protein influences its hinge region. We suggest a mechanism by which T43I may accelerate the development of Alzheimer’s disease in affected patients.

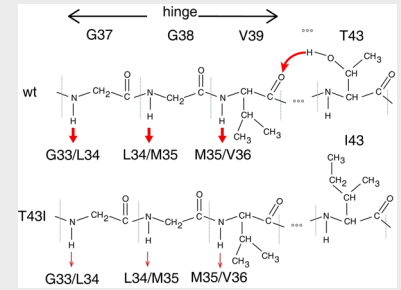

*Walter Stelzer, Christina Scharnagl, Ulrike Leurs, Kasper D. Rand, and Dieter Langosch**

Page No. – Page No.

The impact of the ‘Austrian’ mutation of the amyloid precursor protein transmembrane helix is communicated to the hinge region